Journal of Sound and Vibration (2000) **232**(5), 917–943
doi:10.1006/jsvi.1999.2770, available online at http://www.idealibrary.com on IDEAL®

THE EFFECTS OF LARGE VIBRATION AMPLITUDES ON THE MODE SHAPES AND NATURAL FREQUENCIES OF THIN ELASTIC SHELLS, PART I: COUPLED TRANSVERSE-CIRCUMFERENTIAL MODE SHAPES OF ISOTROPIC CIRCULAR CYLINDRICAL SHELLS OF INFINITE LENGTH

F. Moussaoui

Université Moulay Ismail, Faculté des Sciences et Techniques Département de Physique BP 509, *Errachidia, Morocco*

R. Benamar

Université Mohammed V, Ecole Mohammadia d'Ingénieurs, Département des E.G.T-LERSIM, BP 765, *Rabat, Morocco*

AND

R. G. White

*Department of Aeronautics and Astronautics, University of Southampton, Highfield, Southampton S*017 1 *BJ, England*

(*Received* 16 *November* 1998, *and in final form* 18 *October* 1999)

The effects of large vibration amplitudes on the first and second coupled radial-circumferential mode shapes of isotropic circular cylindrical shells of infinite length are examined. A theoretical model based on Hamilton's principle and spectral analysis developed previously for clamped–clamped beams and fully clamped rectangular plates is extended to shell type structures, reducing the large-amplitude free vibration problem to the solution of a set of non-linear algebraic equations. The transverse and circumferential displacements are assumed to be harmonic and expanded in the form of a finite series of functions. The Donnel–Mushtarie shell theory, taking into account the coupling between extensional and flexural deformations is used. Then, the non-linear deformation energy is expressed by taking into account the non-linear term due to the considerable stretching of the middle surface of the shell induced by large deflections. Tables of numerical results are given for the first and second non-linear modes, for a wide range of the vibration amplitude, which may be used for engineering purposes. For each value of the vibration amplitude considered, the corresponding contributions of the basic functions defining the non-linear transverse and circumferential displacement shapes are given, with the corresponding non-linear frequencies. Selected plots of mode shapes and bending stress distributions are presented, with an extensive discussion of the effects of non-linearity on the dynamic behaviour of shells.

1. INTRODUCTION

The dynamic characteristics of circular cylindrical shells are of practical importance in many branches of engineering, including aerospace engineering and transport vehicle

0022-460X/00/200917 + 27 $35.00/0

design, because of their extensive use in aircraft, commercial vehicles and road tankers. Knowledge of these characteristics is necessary for ensuring the structural integrity of the vehicle and estimating the fatigue life of the structure [1]. Finite circular cylinders are commonly used as ultrasonic transducers and resonators; the natural frequency spectrum of such cylinders has to be calculated accurately for practical purposes [2]. Arnold and Warburton initially presented the widely used equation of motion of thin, unstiffened cylindrical shells by making use of Lagrange's equations with appropriate strain and kinetic energy expressions [3, 4]. This work was confined to cylindrical shells with clamped ends. Coupry presented a theoretical and experimental study in which a simplified formula, applicable in most cases, was developed in order to determine simply the vibratory characteristics of thin cylinders [5]. The free vibration of laminated orthotropic simply supported cylindrical shells has been investigated by Dong [6] and Donnell-type displacement equations of equilibrium, and the natural frequencies have been obtained by an iterative procedure. Bert *et al.* determined the free vibration characteristics of thin-walled cylindrical shells with layers made of an arbitrarily laminated anisotropic elastic material [7]. Subsequently, Warburton and Higgs have extended their work and have used an energy method in conjunction with the Raleigh–Ritz technique to determine the natural frequencies of clamped–free cantilevered cylindrical shells [8]. A universal formula based on Lagrange's equations has been developed by Au–Yang for predicting the natural frequencies, both in air and in a fluid, of thin-walled cylinders and cylindrical panels with either simply supported or clamped boundary conditions [9]. Mayers and Wrenn studied the influence of non-linear effects on the free vibration of thin circular cylindrical shells by using both the Karman–Donnell theory and a modified set of the Senders strain displacement relation, in which an approximate solution has been obtained by means of the direct variational approach for large and small number of circumferential waves [10]. A series of references on the non-linear characteristics of large vibration amplitudes of cylindrical shells covering a period of time from 1961 to 1979 is given in a paper of Ueda [11]. An overview of the subject of non-linear vibration of plates and shells has been given by Leissa [12], who suggested that the main difficulty lies in the solution of the governing equations of motion, which are coupled non-linear differential equations. Tedesco *et al.* have developed an analytical procedure which accurately predicts the natural frequencies and radial mode shapes, based on the numerical investigation of the free vibration of cylindrical shells [13]. This procedure has been applied to a cylindrical tank uniformly attached to a rigid base, with or without a top closure. Thick shells of revolution have been analysed for their axisymmetric vibration behaviour using the theory proposed in [14]. The solution of the problem has been obtained by using a higher order axisymmetric finite element. The asymptotic method has been applied by Koga and Kodama to the free vibration of a circular cylindrical shell under a uniform pressure [15]. This study has led to a simple formula for a natural frequency, which is valid for all possible combinations of the boundary conditions characterizing simply supported, clamped and free ends. Theoretical and experimental investigations of the vibration characteristics of thin-walled ring-stiffened circular cylinders have been presented in reference [16]. The theoretical investigation was based also on the finite element method and compared with experimental results. The Ritz minimum energy approach was applied to study the free vibration of a doubly-tapered cylindrical shallow shell [17]. The same method was employed to examine the natural frequency and vibratory characteristics of doubly curved shallow shells [18]. The Ritz method was further applied by Liew *et al.* in a series of papers, to study free vibration of cantilevered cylindrical shells [19], solid cylinders [20], elastic solids [21], hollow cylinders [22] and elliptical bars [23]. The variational principle has been used to study the free vibration of a structure consisting of a finite cylindrical shell closed at the end by a circular

plate [24]. The eigenvalue equation was resolved by the Rayleigh–Ritz method. Kobayashi and Leissa have derived the governing equations for non-linear vibration of a doubly curved thick shallow shell based upon the first order shear deformation theory and Galerkin's procedure [25]. Recently, a excellent survey on vibration of shallow shells has been reported by Liew *et al.* [26] which summarizes papers published up to 1996.

We can conclude from this brief literature survey that in spite of considerable research, no exact solution for the complicated problem of non-linear vibrations of shells is available which may allow all, or at least most, of the known non-linear effects to be described in a unified manner. In particular, in most of the non-linear theoretical studies, the single-mode solution has been assumed (see, e.g., references 8, 11, 25]). This assumption has been shown both theoretically and experimentally to be inaccurate for beams in references [27, 28], and for homogeneous and laminated plates in reference [29]. A theoretical model based on Hamilton's principle and spectral analysis was developed by Benamar *et al.* in order to adapt the Rayleigh–Ritz linear eigenvalue problem to non-linear problems of thin straight structures [30]. This model was applied to simply supported and fully clamped beams and extended to rectangular isotropic and laminated plates [31, 32]. The purpose of the present paper is to extend this model to shell-type structures, using a multi-mode approach, to investigate the effects of non-linearity on shell dynamic behaviour at large vibration amplitudes. In this paper, which is Part I of a series of papers concerned with non-linear vibration of shells, the case of a circular cylindrical shell of infinite length is examined using a simple mathematical model based on the plane strain assumption [33] and a multi-mode approach. The results obtained using such a model can apply to a cylindrical shell, sufficiently long so that the distance between its longitudinal nodes is much greater than its radius, and consequently, the boundary conditions at the ends of the cylinder do not significantly influence the solution. Harmonic motion was assumed and the transverse and circumferential displacements have been expanded in the form a series of basic functions. After discretization, an expression has been derived for the strain energy at large transverse and circumferential vibration amplitudes. In this expression, in addition to the classical mass and rigidity tensors associate with transverse and circumferential vibrations, 2 third order tensors and 1 fourth order tensor appeared due to the non-linearity. This fact makes the shell problem formulation more complicated compared with the plate case, in which only a fourth order tensor appears due to the non-linearity [27–32]. The dynamic variational problem obtained by applying Hamilton's principle is transformed into a static case by integrating the time functions over a period of vibration (see details below). Minimization of the energy functional with respect to the transverse and circumferential basic functions contributions has led to two coupled sets of non-linear algebraic equations, which have been solved numerically in each case, leading to the first and second non-linear coupled transverse and circumferential mode shapes, each mode being given as a function of the maximum transverse and circumferential amplitude of vibration and the corresponding frequency. The results obtained via the above model, are discussed and compared with those from previous studies. Also, plots of the mode shapes and the associated bending stress distributions obtained at large vibration amplitudes are given, showing a higher rate of increase of stresses with vibration amplitude, compared with that predicted in the linear theory.

2. ANALYTICAL FORMULATION

2.1. PROBLEM DEFINITION

The co-ordinate system and diagram illustrating the parameters used in the model are shown in Figure 1. The structure consists of a circular cylindrical shell with radius and

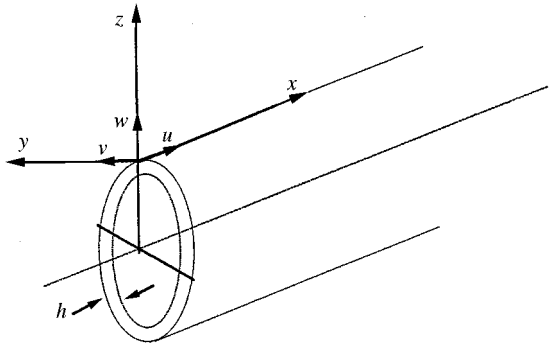

Figure 1. Schematic diagram of a circular cylindrical shell.

thickness denoted as R and h. The shell is composed of an elastic, homogenous isotropic material, and is assumed to be thin, that is, its wall thickness is less than 10% of its radius [9]. The shell motion is represented by V and W, which are the displacements in the tangential and radial directions respectively.

Rotary inertia and shear deformation are neglected, and, there is no external load applied to the shell. Therefore, the conventional assumptions of the Donnel–Mushtarie shell theory are adopted. The concept of strain plane is considered in this study. It is assumed that there is no motion in the longitudinal direction of the shell, and that the physical quantities (displacement, membrane forces, bending moments, etc.) do not depend upon location along the length. Taking into account these assumptions, the strain–displacement relationships can be written as

$$\varepsilon_x = 0, \quad \varepsilon_y = \varepsilon_y^0 - z\kappa_y, \quad \varepsilon_{xy} = 0 \tag{1}$$

where ε_i^0 $(i = x, y, z)$ and κ_y are the in-plane strains at the shell mid-surface and the bending curvatures respectively, and given by

$$\varepsilon_y^0 = \frac{\partial V}{\partial y} + \frac{W}{R} + \frac{1}{2}\left(\frac{\partial W}{\partial y}\right)^2 \tag{2}$$

and

$$\kappa_y = \frac{\partial^2 W}{\partial y^2}. \tag{3}$$

2.2. THE BENDING STRAIN, AXIAL STRAIN AND KINETIC ENERGIES OF A SHELL

The total strain energy, V, of the shell described above is composed of the membrane energy V_m and the bending strain energy V_b,

$$V = V_m + V_b. \tag{4}$$

The membrane strain energy is caused by the stretching effects of the mid-surface of the shell. The strain energy components have been deduced from the general expression given in

reference [34] as

$$V_m = \frac{6D}{h^2}\int_x\int_y [\![(\varepsilon_y^0)^2]\!]\,\mathrm{d}x\,\mathrm{d}y$$

$$V_b = \frac{D}{2}\int_x\int_y \{(\Delta W)^2\}\,\mathrm{d}x\,\mathrm{d}y \tag{5}$$

in which D is the flexural rigidity $D = Eh^3/12\,(1-\nu^2)$, E is Young's modulus, ν is Poisson's ratio, and Δ is the Laplacian operator defined as $(\partial^2/\partial x^2 + \partial^2/\partial y^2)$.

Substituting equations (2) and (3) into equations (5) and (4), we find the total energy expression:

$$V = \frac{6D}{2h^2}\int_y \left[\frac{1}{4}\left(\frac{\partial W}{\partial y}\right)^4 + \left(\frac{\partial V}{\partial y}\right)\left(\frac{\partial W}{\partial y}\right)^2 + \frac{W}{R}\left(\frac{\partial W}{\partial y}\right)^2 + \left(\frac{W}{R}\right)^2 + 2\frac{W}{R}\left(\frac{\partial V}{\partial y}\right) + \left(\frac{\partial V}{\partial y}\right)^2\right]\mathrm{d}y$$

$$+ \frac{D}{2}\int_y \left(\frac{\partial^2 W}{\partial y^2}\right)^2 \mathrm{d}y \tag{6}$$

and the kinetic energy is given by

$$T = \frac{\rho h}{2}\int_y \left[\left(\frac{\partial V}{\partial t}\right)^2 + \left(\frac{\partial W}{\partial t}\right)^2\right]\mathrm{d}y, \tag{7}$$

where ρ is the mass per unit volume.

2.3. DISCRETIZATION OF THE TOTAL STRAIN AND KINETIC ENERGY EXPRESSIONS

If the time and space functions are supposed to be separable and harmonic motion is assumed, the circumferential and transverse displacement functions can be written as

$$V(y,t) = V(y)\cos\omega t,$$

$$W(y,t) = W(y)\cos\omega t. \tag{8}$$

Using a multi-mode approach, $V(y)$ and $W(y)$ are expanded in the form of finite series as

$$V(y) = B_i V_i(y),$$

$$W(y) = C_j W_j(y), \tag{9}$$

in which the usual summation convention is used, according to which summation is made for the repeated indices i and j over the range $[1, n]$.

Discretization of the total strain energy and the kinetic energy expressions is achieved by substituting equation (9) into equations (6) and (7), and rearranging. We then obtain the following relationship:

$$V = \tfrac{1}{2}C_iC_jC_kC_l b_{ijkl}\cos^4\omega t + \tfrac{1}{2}C_iC_jC_k b^1_{ijk}\cos^3\omega t + \tfrac{1}{2}C_iC_jB_k b^2_{ijk}\cos^3\omega t$$

$$+ \tfrac{1}{2}B_iB_j k^1_{ij}\cos^2\omega t + \tfrac{1}{2}C_iC_j k^2_{ij}\cos^2\omega t + \tfrac{1}{2}C_iB_j k^3_{ij}\cos^2\omega t, \tag{10}$$

where b_{ijkl}, and b^1_{ijk} and b^2_{ijk} are a fourth order and 2 three order non-linearity tensors, and k^1_{ij}, k^2_{ij} and k^3_{ij} are the rigidity tensors, associated with V, W and the coupling between V and W respectively. The vibration parameters are given by the following expressions:

$$b_{ijkl} = \frac{12D}{h^2} \int_0^{\pi R} \frac{1}{4} \frac{\partial W_i}{\partial y} \frac{\partial W_j}{\partial y} \frac{\partial W_k}{\partial y} \frac{\partial W_l}{\partial y} \mathrm{d}y,$$

$$b^1_{ijk} = \frac{12D}{h^2 R} \int_0^{2\pi R} \frac{\partial W_i}{\partial y} W_k \mathrm{d}y,$$

$$b^2_{ijk} = \frac{12D}{h^2} \int_0^{2\pi R} \frac{\partial W_i}{\partial y} \frac{\partial W_j}{\partial y} \frac{\partial V_k}{\partial y} \mathrm{d}y,$$

$$k^1_{ij} = \frac{12D}{h^2} \int_0^{2\pi R} \frac{\partial V_i}{\partial y} \frac{\partial V_j}{\partial y} \mathrm{d}y,$$

$$k^2_{ij} = \frac{12D}{h^2} \int_0^{2\pi R} \left[\frac{W_i W_j}{R^2} + \frac{h^2}{12} \frac{\partial^2 W_i}{\partial y^2} \frac{\partial W_j}{\partial y^2} \right] \mathrm{d}y,$$

$$k^3_{ij} = \frac{12D}{h^2 R} \int_0^{2\pi R} 2 W_i \frac{\partial V_i}{\partial y} \mathrm{d}y. \tag{11}$$

The discretized expression for the kinetic energy is obtained by substituting equations (9) into equation (7), which leads to

$$T = \left[\frac{1}{2} B_i B_j m^1_{ij} + \tfrac{1}{2} C_i C_j m^2_{ij} \right] \omega^2 \sin^2 \omega t, \tag{12}$$

in which m^1_{ij} and m^2_{ij} are the mass tensors associated with V and W respectively, given by

$$m^1_{ij} = \rho h R \int_0^{2\pi R} V_i V_j \mathrm{d}y,$$

$$m^2_{ij} = \rho h R \int_0^{2\pi R} W_i W_j \mathrm{d}y. \tag{13}$$

2.4. FORMULATION OF GOVERNING EQUATIONS

The dynamic behaviour of the structure is governed by Hamilton's principle, which is symbolically written as

$$\delta \int_{t_1}^{t_2} (V - T) = 0. \tag{14}$$

After replacing V and T by their discretized expressions in equation (14), the time functions have to be integrated. The range of integration was chosen equal to $[0, \pi/2\omega]$ which

corresponds to a quarter of a period of motion. This choice was made in order to avoid obtaining zero as the coefficient of the terms involving the third order tensors b^1_{ijk} and b^2_{ijk}, as would have happened if the range of integration was $[0, \pi/\omega]$ or $[0, 2\pi/\omega]$. The variational problem reduces to $\delta\Phi = 0$, in which Φ is a function of the undetermined coefficients B_i and C_i defined by

$$\Phi = \frac{\pi}{2\omega}\left[\frac{3}{8}C_iC_jC_kC_lb_{ijkl} + \frac{2}{3\pi}(C_iC_jC_kb^1_{ijk} + C_iC_jB_kb^2_{ijk}) + \frac{1}{2}(B_iB_jk^1_{ij} + C_iC_jk^2_{ij} + C_iB_jk^3_{ij})\right.$$

$$\left. - \frac{1}{2}(B_iB_jm^1_{ij} + C_iC_jm^2_{ij})\omega^2\right]. \tag{15}$$

The problem is to find the minimum of the function Φ with respect to the unknown coefficients B_i and C_i representing the contribution of the chosen basic functions to the circumferential and transverse displacements V and W, respectively. This is obtained by writing

$$\frac{\partial\Phi}{\partial B_r} = 0, \qquad \frac{\partial\Phi}{\partial C_s} = 0 \quad (\text{with } r, s = 1, \ldots, n). \tag{16}$$

Generally, and this is the case in the present work, the tensors k_{ij} and m_{ij} are symmetric, and the fourth order tensor b_{ijkl} is such that

$$b_{ijkl} = b_{klij}, \qquad b_{ijkl} = b_{jilk} \tag{17}$$

and the third order tensors b^1_{ijk} and b^2_{ijkl} are such that

$$b^1_{ijk} = b^1_{kij}, \qquad b^2_{ijk} = b^2_{jik}.$$

Taking into account these properties of symmetry, it appears that equations (16) are equivalent to

$$\frac{2}{3\pi}C_iC_jb^2_{ijr} + B_ik^1_{ir} + \tfrac{1}{2}C_ik^3_{ir} - \omega^2B_im^1_{ir} = 0, \quad r = 1, \ldots, n \tag{18}$$

$$\frac{3}{2}C_iC_jC_kb_{ijks} + \frac{2}{\pi}C_iC_jb^1_{ijs} + \frac{4}{3\pi}C_iB_jb^2_{ijs} + C_ik^2_{is} + \frac{1}{2}B_ik^3_{is} - \omega^2C_im^2_{is} = 0, \quad s = 1, \ldots, n.$$

This is a set of $2n$ non-linear algebraic equations which has to be solved numerically in order to obtain the non-linear free response of the shell at large vibration amplitudes.

2.5. BENDING, AXIAL AND TOTAL STRESS EXPRESSIONS

By using the classical thin shell assumption of plane strain and Hooke's law, the maximum total stress can be obtained for the external circumference of the cylinder, i.e., $z = h/2$, as

$$\sigma_{yyt} = \sigma_{yyu} + \sigma_{yyb}, \tag{19}$$

where σ_{yya} is the axial stress given by

$$\sigma_{yya} = \frac{E(1-\nu)}{(1+\nu)(1-2\nu)}\left[\frac{\partial V}{\partial y} + \frac{W}{R} + \frac{1}{2}\left(\frac{\partial W}{\partial y}\right)^2\right] \tag{20}$$

and σ_{yyb} is the maximum bending stress given by

$$\sigma_{yyb} = -\frac{E(1-\nu)}{(1+\nu)(1-2\nu)}\frac{h}{2}\left[\frac{\partial^2 W}{\partial y^2}\right]. \tag{21}$$

3. DISCUSSION OF THE NUMERICAL MODEL AND NON-DIMENSIONAL FORMULATION

3.1. DISCUSSION OF THE NUMERICAL MODEL

Equation (18) represent a set of $2n$ non-linear equations relating the n coefficients B_i, the n coefficients C_i and the frequency ω. So we have $(2n+1)$ unknowns and $2n$ equations. In order to complete the formulation, a further equation has to be added to equation (18). As no dissipation is considered here, such an equation can be obtained by applying the principle of conservation of energy, which can be written as

$$V_{max} = T_{max}, \tag{22}$$

where V_{max} is the maximum value of the strain energy obtained from equation (10) for $t = 0$, at which $T = 0$, and T_{max} is the maximum value of kinetic energy obtained from equation (12) for $t = \pi/2\omega$, at which $V = 0$. Equation (22) leads to the following expression for ω^2:

$$\omega^2 = \frac{C_i C_j C_k C_l b_{ijkl} + C_i C_j C_k b^1_{ijk} + C_i C_j B_k b^2_{ijk} + B_i B_j k^1_{ij} + C_i C_j k^2_{ij} + C_i B_j k^3_{ij}}{B_i B_j m^1_{ij} + C_i C_j m^2_{ij}} \tag{23}$$

which has to be substituted into equations (18) to obtain a system of non-linear algebraic equations whose solution leads to the n contribution coefficients B_i, $i = 1, \ldots, n$, corresponding to the circumferential displacement V, and the n contribution coefficients C_i, $i = 1$–n, corresponding to the transverse displacement W.

Adapting the solution procedure used in references [28–32], the technique adopted in the present work was to solve equations (18) assuming a given value C_{s_0} of the contribution coefficient of the function W_{s_0} in order to determine the contribution coefficients C_i of the functions W_i $(i \neq s_0)$ and B_i, $i = 1$–n, of the functions V_i $(i = 1$–$n)$ respectively. The values of C_i $(i \neq s_0)$ and B_i $(i = 1$–$n)$, obtained by solving equations (18) can be substituted into equation (23) to obtain the corresponding value of $\omega^2_{s_0}$. Such a procedure, starting by fixing C_{s_0}, leads to a coupled transverse circumferential mode, which is W dominant. A similar procedure can be adopted when fixing the contribution coefficients B_{r_0} in order to obtain the corresponding non-linear mode, which would be in this case V dominant, with the associated non-linear frequency. Because of the coupling between the shell circumferential and radial displacements, a given shell mode shape is composed of a given function for the radial displacements W together, with the corresponding function for the circumferential displacements V. From a study of linear results obtained previously [33, pp. 41–43], and numerical results obtained here for the non-linear case, it can be seen that the radial and circumferential displacement functions corresponding to a given mode have the same

wavenumber n. However, for a given value of the wavenumber n, there are two associated modes, defined by two frequencies and two values of the amplitude ratio, i.e., C/B. For example, for the apparent first mode there are two modes, defined by two frequencies, designated in the remainder of this paper as the lowest and the highest frequency as in reference [33, p. 44], for which the amplitude ratios of the corresponding W and V functions are -1 and $+1$ respectively. So, in this case, the modes cannot be said to be predominately circumferential or radial in nature. But when the mode order increases, the ratio of the W and V function amplitudes C/B, corresponding to the lowest frequency, decreases, leading to a shell mode shape which is predominately radial. But the ratio of the W and V function amplitudes, corresponding to the highest frequency, increases, leading to a shell mode shape which is predominately circumferential. As will be shown later, the numerical results obtained here in the non-linear case, are both qualitatively and quantitatively in very good agreement with the shell mode shape behaviour, described above, known in linear theory.

3.2. NON-DIMENSIONAL FORMULATION

To simplify the analysis and the numerical treatment of the set of non-linear algebraic equations, non-dimensional formulation has been considered by putting the displacement functions as

$$V_i(y) = hV_i^*(y^*),$$

$$W_i(y) = hW_i^*(y^*), \tag{24}$$

where $y^* = y/R$ is the non-dimensional co-ordinate. Equation (18) can be rewritten in non-dimensional form as

$$\frac{2}{3\pi} C_i C_j b_{ijr}^{*2} + B_i k_{ir}^{*1} + \tfrac{1}{2} C_i k_{ir}^{*3} - \omega^2 B_i m_{ir}^{*1} = 0,$$

$$\frac{3}{2} C_i C_j C_k b_{ijks}^* + \frac{2}{\pi} C_i C_j b_{ijs}^{*1} + \frac{4}{3\pi} C_i B_j b_{ijs}^{*2} + C_i k_{is}^{*2} + \frac{1}{2} B_i k_{is}^{*3} - \omega^{*2} C_i m_{is}^{*2} = 0 \tag{25}$$

where ω^* is the non-dimensional non-linear frequency parameter defined by

$$\omega^2 = \frac{12D}{\rho h^3 R^2} \omega^{*2} \tag{26}$$

in which ω^{*2} is given by the following expression:

$$\omega^{*2} = \frac{C_i C_j C_k C_l b_{ijkl}^* + C_i C_j C_k b_{ijk}^{1*} + C_i C_j B_k b_{ijk}^2 + B_i B_j k_{ij}^{1*} + C_i C_j k_{ijk}^{2*} + C_i B_j k_{ij}^{3*}}{B_i B_j m_{ij}^{1*} + C_i C_j m_{ij}^{2*}}. \tag{27}$$

The b_{ijkl}^*, b_{ijk}^{1*}, b_{ijk}^{2*}, k_{ij}^{1*}, k_{ij}^{2*}, k_{ij}^{3*}, m_{ij}^{1*} and m_{ij}^{2*} terms are non-dimensional tensors related to the dimensional ones by the following equations:

$$b_{ijkl} = \frac{12D}{R} b_{ijkl}^*, \qquad b_{ijk}^1 = \frac{12D}{R} b_{ijk}^{1*}, \qquad b_{ijk}^2 = \frac{12D}{R} b_{ijk}^{2*},$$

$$k^1_{ijk} = \frac{12D}{R}\, k^{1*}_{ijk}, \qquad k^2_{ijk} = \frac{12D}{R}\, k^{2*}_{ijk}, \qquad k^3_{ijk} = \frac{12D}{R}\, k^{3*}_{ijk},$$

$$m^1_{ir} = \rho h^3 R m^{1*}_{ir}, \qquad m^2_{is} = \rho h^3 R m^{2*}_{is}. \tag{28a}$$

The non-dimensional tensors are defined by

$$b_{ijkl} = \frac{\beta^2}{4} \int_0^{2\pi} \frac{\partial W^*_i}{\partial y^*} \frac{\partial W^*_j}{\partial y^*} \frac{\partial W^*_k}{\partial y^*} \frac{\partial W^*_l}{\partial y^*}\, \mathrm{d}y^*,$$

$$b^{1*}_{ijk} = \beta \int_0^{2\pi} \frac{\partial W^*_i}{\partial y^*} \frac{\partial W^*_j}{\partial y^*}\, W^*_k\, \mathrm{d}y^*,$$

$$b^{2*}_{ijk} = \beta \int_0^{2\pi} \frac{\partial W^*_i}{\partial y^*} \frac{\partial W^*_j}{\partial y^*} \frac{\partial V^*_k}{\partial y^*}\, \mathrm{d}y^*, \tag{28b}$$

$$k^{1*}_{ij} = \int_0^{2\pi} \frac{\partial V^*_i}{\partial y^*} \frac{\partial V^*_j}{\partial y^*}\, \mathrm{d}y^*,$$

$$k^{2*}_{ij} = \int_0^{2\pi} \left[W^*_i W^*_j + \frac{\beta^2}{12} \frac{\partial^2 W^*_i}{\partial y^{*2}} \frac{\partial^2 W^*_j}{\partial y^{*2}} \right] \mathrm{d}y^*,$$

$$k^{3*}_{ij} = 2 \int_0^{2\pi} W^*_i \frac{\partial V^*_i}{\partial y^*}\, \mathrm{d}y^*$$

and

$$m^{1*}_{ij} = \int_0^{2\pi} V^*_i V^*_j\, \mathrm{d}y^*,$$

$$m^{2*}_{ij} = \int_0^{2\pi} W^*_i W^*_j\, \mathrm{d}y^*. \tag{29}$$

The parameters b_{ijkl}, b^1_{ijk}, b^2_{ijk}, k^1_{ij}, k^2_{ij}, k^3_{ij}, m^1_{ij} and m^2_{ij} given by equations (11) and (13) depend only on the geometrical parameter $\beta = h/R$, Poisson's ratio ν and the chosen basic functions V^*_i and W^*_i. Also, it should be noticed that the non-linear frequency parameter ω^* does not depend on the Poisson ratio, since none of the parameters b^*_{ijkl}, b^{1*}_{ijk}, b^{2*}_{ijk}, k^{1*}_{ij}, k^{2*}_{ij}, k^{3*}_{ij}, m^{1*}_{ij} and m^{2*}_{ij} is a function of ν, but the non-linear frequency itself depends in all cases on ν, via the shell bending stiffness $D = Eh^3/12(1-\nu^2)$, as shown in equation (26).

In terms of the non-dimensional parameters defined in the previous equations, non-dimensional axial, bending and total stresses σ^*_{yya}, σ^*_{yyb} and σ^*_{yyt} can be defined respectively, by

$$\sigma^*_{yya} = \left[\beta \left(\frac{\partial V^*}{\partial y^*} + \frac{W^*}{R} \right) + \frac{\beta^2}{2} \left(\frac{\partial W^*}{\partial y^*} \right)^2 \right], \tag{30}$$

$$\sigma^*_{yyb} = -\frac{\beta^2}{2} \left[\frac{\partial^2 W^*}{\partial y^{*2}} \right] \tag{31}$$

and

$$\sigma_{yyt} = \sigma_{yya} + \sigma_{yyb}. \tag{32}$$

The relationships between the dimensional and the non-dimensional stresses are

$$\sigma_{a,b \text{ and } t} = \frac{E(1-\nu)}{(1+\nu)(1-2\nu)} \sigma^*_{a,b \text{ and } t} \tag{33}$$

In the case of plain strain, the equations describing the free vibrations of cylindrical shells admit solutions which are independent of the axial co-ordinate x^* and may be expanded in the form of finite series as follows:

$$\begin{aligned} U^*(y^*, t) &= 0, \\ V^*(y^*, t) &= (B_i/h)\sin(iy^*)\cos(\omega t), \\ W^*(y^*, t) &= (C_i/h)\cos(jy^*)\cos(\omega t), \end{aligned} \tag{34}$$

in which the usual summation assumption is assumed.

Equations (34) were substituted in a FORTRAN program for studying the non-linear dynamic behaviour of an infinitely long circular cylindrical shell as previously discussed.

4. NUMERICAL RESULTS AND DISCUSSION

4.1. NUMERICAL DETAILS

It appears clearly from the set of non-linear algebraic equations (25) that the radial and circumferential displacements are coupled via the second order tensor k^{2*}_{ij} and the third order tensor b^{2*}_{ijk}. These equations have been solved numerically using the Harwell library routine NS01A. This routine is based on a hybrid iteration method combining the step descent and Newton's methods which do not require a very good initial estimate of the solution [35]. A step procedure, similar to that described in references [29–31] for beams and plates, was adopted for ensuring rapid convergence when varying the amplitude, which allowed solutions to be obtained with quite a small number of iterations (an average of 100 for 12 equations). So, to obtain the lowest frequency parameter corresponding to the predominately transverse sth non-linear mode shape, the first calculation was done in the neighbourhood of the linear solution by attributing a small numerical value to the coefficient C_s of the basic function W^*_s. The resulting solution was used as an initial estimate for the following step corresponding to $C + \Delta C$. Thus, by choosing in each case the convenient value of the step ΔC, the sth non-linear coupled radial-circumferential mode shape, for which the motion is primarily transverse, has been calculated at various maximum vibration amplitude to shell thickness ratios extending up to a given value. The same procedure was applied to obtain the highest frequency parameter corresponding to a motion which is predominately circumferential. So, the rth non-linear mode shape was calculated by attributing a small numerical value to the coefficient B_r of the basic function V^*_r.

4.2. CONVERGENCE OF THE SPECTRAL EXPANSION

A step procedure, similar to that described above, was used to cover the desired range of amplitudes. The limit of error residuals was imposed to be lower than 10^{-16} in all cases. To obtain the fundamental and second non-linear mode shapes of the shell considered above, the first 12 basic functions $(w_1^*, w_2^*, \ldots, w_{12}^*)$ associated with the transverse displacement W^* and 12 basic functions $(v_1^*, v_2^*, \ldots, v_{12}^*)$ associated with the circumferential displacement V^* were used in the series expansions (34), which leads to the solution of 23 non-linear algebraic equations.

Typical values of the coefficients C_i and B_i are given in Table I (as an example) for the lowest second mode. It can be seen that the only significant contributions, as may be expected due to the symmetry of the shell second mode shape, are those corresponding to the basic functions $W^*(y^*) = (C_i/h)\cos(iy^*)$ and $V^*(y^*) = (B_i/h)\sin(iy^*)$, in which i is an odd number for the second mode. To check that the addition of symmetric functions does not affect the results, calculations were made with only six functions for W^* and six functions for V^* representing the shape of each mode considered. The results show no significant change in both the value of the resonance frequencies and the basic function contributions. So the conclusion has been reached that good estimates of the non-linear mode shapes can be obtained by solving only 11 equations corresponding to 12 well chose basic functions for W and V.

TABLE 1

Lowest second non-linear mode shape when the motion is predominately transverse, for $\beta = 0{\cdot}05$. *Typical numerical results obtained with* 23 *basic functions*

W^*_{max}	0·02766874	0·62406954	1·28088628
ω^*_{nl}/ω^*_l	1·002283	2·04357	3·147069
C_2	0·50000000E − 05	1·3000000000	2·5500000000
C_1	− 0.13792493E − 05	− 0.23615902E − 13	− 0.23042550E − 13
C_3	0.10415065E − 06	0.15919448E − 13	0.12312677E − 13
C_4	− 0.59071467E − 03	− 0.23994920E + 00	− 0.38325542E + 00
C_5	0·68004758E − 08	− 0·59431545E − 14	− 0·53068146E − 14
C_6	0·86744433E − 05	0·69523074E − 01	0·17056876E + 00
C_7	− 0.19261279E − 09	0·27232039E − 14	0·34736108E − 14
C_8	− 0.14127602E − 06	− 0.23127118E − 01	− 0·70534312E − 01
C_9	− 0·20345207E − 09	− 1·13134491E − 14	− 0·21023490E − 14
C_{10}	0·23176058E − 08	0·82245200E − 02	0·33834075E − 01
C_{11}	0·30596649E − 09	0·61410704E − 15	0·13077928E − 14
C_{12}	0·20926962E − 09	− 0·30620594E − 02	− 0·17174141E − 01
B_1	0·13798122E − 05	0·23633729E − 13	0·22892653E − 13
B_2	− 0·25016762E − 01	− 0·65181445E + 00	− 0·12834731E + 01
B_3	− 0·34631815E − 07	− 0·51816889E − 14	− 0·38651361E − 14
B_4	0·14021889E − 03	0·54967182E − 01	0·76477320E − 01
B_5	− 0·15464522E − 08	0·99580161E − 15	0·75988544E − 15
B_6	− 1·12100725E − 05	− 0·91002461E − 02	− 0·20642792E − 01
B_7	0·32992351E − 09	− 0·27727641E-15	− 0·31175795E − 15
B_8	0·11555313E − 07	0·17349761E − 02	0·40335935E − 02
B_9	− 0·45226507E − 10	0·91329420E − 16	0·11809233E − 15
B_{10}	− 0·52934915E − 09	− 0·29485056E − 03	− 0·72168979E − 02
B_{11}	− 0·11630189E − 11	− 0·36275615E − 16	− 0·53893769E − 16
B_{12}	− 0·23193377E − 09	0·16512369E − 04	− 0·12240708E − 03

4.3. COMPARISON WITH LINEAR RESULTS

In order to validate the theory and the numerical results obtained in the present work, comparison is made in this section between results obtained here from the non-linear model when the vibration amplitudes considered are very small and data from other analyses: (a) previous results from a linear analysis corresponding to infinitely long cylindrical shells [33, pp. 41, 39], (b) results obtained from the general model developed here when the non-linearity tensors b^{*1}_{ijk}, b^{*2}_{ijk} and b^{*}_{ijkl} are neglected, and (c) previous results of linear analyses corresponding to very long cylindrical shells with various boundary conditions, the shells being considered long enough to allow comparison to be made with present work [33, pp. 43, 47, 59).

Tables 2–4 show a comparison of numerical results obtained from the solution of the set of non-linear algebraic equations (25), corresponding to the non-linear problem, obtained for

TABLE 2

Comparison of non-dimensional frequency parameters of the coupled radial–circumferential modes, obtained here for small amplitudes, with previous linear results, for various mode orders: (*a*) *values published in reference* [33, *p.* 41] *or calculated from equation* (12-10) *of reference* [33, *p.* 39], (*b*) *values obtained from solution of the set of linear algebraic equations of the present work, when the non-linear tensors* b^{*}_{ijkl}, b^{*1}_{ijk} and b^{*2}_{ijk} *are omitted*, (*c*) *values obtained from solution of the set of non-linear algebraic equations* (25) *of the present analysis*, (*d*) *values published in reference* [33, *pp.* 47, 59] *according to Flügge's linear theory for a very long shell* ($L/mR = 100$, *with* $m = 1$) *supported at both ends by shear diaphragm* (*SD-SD*)

$\beta = 0{\cdot}05$	Mode order	(a)	(b)	(c)	(d)
Highest	First	1·41425	1·41425	1·41425	1·41440
Frequency ω_c^*	Second	2·23622	2·23622	2·23622	2·23628
Lowest	First	1·02062E − 02	1·02062E − 02	1·02151E − 02	—
Frequency ω_r^*	Second	5·16417E − 02	5·16363E − 02	5·17537E − 02	—

TABLE 3

Comparison of vibration amplitude ratios, for small amplitudes and various mode orders, with previous linear results for coupled radial–circumferential modes: (*a*) *values computed from equation* (2.32) *published in reference* [33, *p.* 43] *in the linear case*, (*b*) *values obtained from solution of the set of linear algebraic equations of the present work, when the non-linear tensors* b^{*}_{ijkl}, b^{*1}_{ijk} *and* b^{*2}_{ijk} *are omitted*, (*c*) *values obtianed from solution of the set of non-linear algebraic equation* (25) *of the present analysis*, (*d*) *values transferred from table* (2.11) *of reference* [33, *p.* 39] *according to Flügge's linear theory for long simply supported shell* ($L/mR = 100$, *with* $m = 1$)

$\beta = 0{\cdot}05$	Mode order	(a)	(b)	(c)	(d)
Amplitude ratios	First	0·99989	1·00000	1·00000	—
$(B/C)_{r_0}$ for the	Second	1·99864	1·99867	1·99867	—
highest frequency					
Amplitude ratios	First	− 1·00000	− 1·00000	− 0·99990	1·03268
$(B/C)_{s_0}$ for the	Second	− 0·50005	− 0·50000	− 0·50000	0·504356
lowest frequency					

TABLE 4

Comparison of non-dimensional lowest frequency parameters obtained here for small amplitudes and various thickness/radius ratios with previous linear results; (*a*) *values computed from equation* (2.31) *published in reference* [33, *p.* 39] *for the linear case*, (*b*) *values obtained from sloution of the set of non-linear algebraic equations* (25) *of the present analysis for* $C_{s_0} = 0{\cdot}05$; $s_0 = 1, 2$ *according to the first and second modes*

$\beta = h/R$	0·001	0·01	0·02	0·03	0·04	0·05
First mode						
(a) ω_l^*	0·204124E − 03	2·041231E − 03	4·082482E − 03	6·123723E − 03	8·164965E − 03	10·206200E − 03
(b) ω_{nl}^*	0·204307E − 03	2·043066E − 03	4·086119E − 03	6·129146E − 03	8·172135E − 03	10·215070E − 03
Second mode						
(a) ω_l^*	1·032795E − 03	10·327962E − 03	20·656035E − 03	30·984285E − 03	$41{\cdot}312819^{E}$ − 03	51·641715E − 03
(b) ω_{nl}^*	1·033720E − 03	10·333126E − 03	20·674144E − 03	31·001515E − 03	$41{\cdot}346983^{E}$ − 03	51·753650E − 03

small vibrations amplitudes, with previous results of linear analyses. The highest frequency ω_c^* and the lowest frequency ω_r^* corresponding to the first and second modes are presented in Table 2 for a thickness to radius ratio β equal to 0·05. The amplitude ratios $(B/C)_{r_0}$ corresponding to these modes are indicated in Table 3 for the same parameters. Results in column (a) of Table 2 are taken from Table (2.2) published in reference [33, pp. 41] or calculated from equation (2.31) given in references [33–35]. Results in column (d) are transferred from Table (2.10) of reference [33, pp. 47, 49], obtained by solution of the linear characteristic equation according to the Flügge theory for a very long circular cylindrical shell having a length to radius ratio equal to 100, supported by shear diapharagrams (SD–SD) at both ends. Results in column (a) of Table 3 are obtained from equation (2.32) presented in reference [33, p. 43]. Results in column (d) of Table 3 are transferred from Table (2.11) of reference [33, p. 39] according to the Flügge theory for a very long simply supported shell for which $L/mR = 20$. The results from references [33, pp. 39, 47, 59] have been obtained by the solution of the set of differential equations of the linear problem corresponding to a circular cylindrical shell of infinite length, according to the Donnel–Mushtarie theory. Results in column (b) of Tables 2 and 3 were obtained from the solution of the set of linear algebraic equations obtained in the present work, with the non-linear tensors b^*_{ijkl}, b^{*1}_{ijk} and b^{*2}_{ijk} omitted. Results in columns (c) of Tables 2 and 3 are obtained from the solution of the set of non-linear algebraic equations of the present analysis for small amplitudes ($B_{r_0} = 0{\cdot}05$ in the case of the highest frequency, and $C_{s_0} = 0{\cdot}05$ in the case of the lowest frequency with $r_0 = 1, 2$ and $s_0 = 1, 2$). It can be seen from all the comparisons mentioned above that both resonance frequencies and amplitude ratios of the coupled transverse–circumferencial mode, obtained from the present non-linear analysis at small vibration amplitudes, are very close to those obtained from linear analyses of the previous studies. Moreover, the agreement between the two sets of results, according to lowest frequency, computed in the linear case (column (a)) and in the non-linear case (column (c)) is very good. Indeed, for most cases, the results agree within 1%. The same observation can be made for amplitude ratio results. It is worth noting here, from the numerical methods point of view, that a classical eigenvalue problem, solved usually by using classical numerical methods, such as Jacobi's method, appears here, as has been pointed out in previous non-linear studies [28–31], as a limit of a non-linear problem, described by a set of non-linear algebraic equations, the solution of which tends to the eigenvalue problem solution when the displacement amplitude tends to zero. In Table 4, the non-linear lowest frequency parameters of the first and second mode shapes obtained here for small amplitudes $C_1 = 0{\cdot}05$ and $C_2 = 0{\cdot}05$ are compared with those obtained from a previous linear analysis in reference [33, p. 39] for various shell thickness to radius ratios, and good agreement can be seen.

4.4. COMPARISON WITH THE NON-LINEAR RESULTS OF THE SINGLE-MODE APPROACH

In order to estimate the accuracy of the non-linear numerical results obtained in the present work, a comparison has been made in Figure 2 between the fundamental non-linear mode found by Chu [36] when $L/R \to \infty$ and that derived here. Unfortunately, the results available in the shell vibration literature are based on the single-mode approach. So, although various techniques have been used, as discussed in the introduction, no results were found for the coefficient contribution dependence of the mode shapes. Consequently, the comparison was restricted to the amplitude dependence of the resonance frequency associated with the fundamental non-linear mode. Good agreement can be seen between the curve of results obtained in this analysis for the fundamental non-linear mode and Chu's

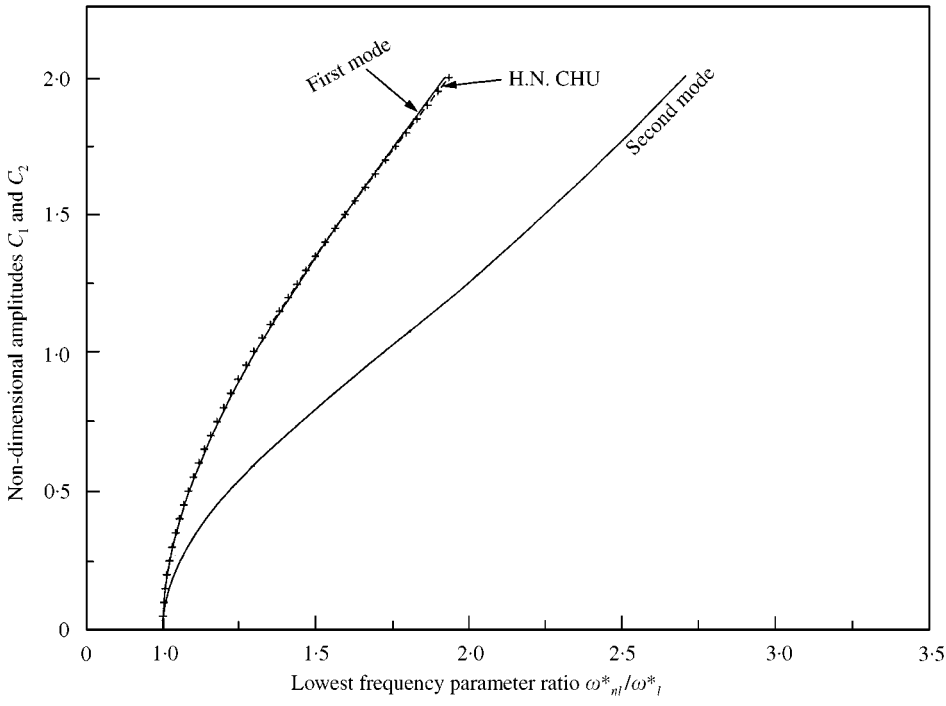

Figure 2. Effects of large vibration amplitudes on the frequencies of the lowest first and second modes. Comparison with previous non-linear studies.

data (Figure 2). This agreement is due to the values of coefficient contributions, obtained by the present analysis, C_3, C_5, C_7, C_9, C_{11}, B_1, B_3, B_5, B_7, B_9 and B_{11} (see Tables 5(a)–(b) and Figure 3) which are quite small for the first mode. Although the contribution coefficients are relatively small, their effects on the non-linear stresses may be quite important, as will be discussed below. As may be expected, due to higher tensile forces induced by the second mode, the coefficient contributions C_4, C_6, C_8, C_{10}, C_{12}, B_2, B_4, B_6, B_8, B_{10} and B_{12} are more important, showing non-linearity effects, which are greater than those obtained for the fundamental non-linear mode. Also, it is interesting to note that these results present a character of non-linearity of the hardening type (i.e., the frequency increases with increasing vibration amplitude) as has been observed by Chu [36], Dowell and Ventres [33, pp. 222–223] for large deflections of a circular cylindrical shell for which $L/R \to \infty$, and by Mayer and Wrenn for long circular cylindrical shell [10].

4.5. GENERAL PRESENTATION OF NUMERICAL RESULTS

Numerical results for a circular cylindrical shell of infinite length and having a thickness to radius ratio β equal to 0·05 are summarized in Tables 5(a), (b) for the first and second mode shapes. In Table 5(a), computed values of C_3, C_5, C_7, C_9, C_{11}, B_1, B_3, B_5, B_7, B_9 and B_{11} corresponding to C_1 varying from 0·05 to 2 are given. Also in Table 5(b), computed values of C_4, C_6, C_8, C_{10}, C_{12}, B_2, B_4, B_6, B_8, B_{10} and B_{12} corresponding to C_2 varying from 0·05 to 2 are given. For each solution C_3, C_5, C_7, C_9, C_{11}, B_1, B_3, B_5, B_7, B_9 and B_{11}, and C_4, C_6, C_8, C_{10}, C_{12}, B_2, B_4, B_6, B_8, B_{10} and B_{12}, the corresponding value of lowest frequency

TABLE 5

Contribution coefficients of transverse and circumferential basic functions corresponding to the lowest first and second non-linear mode shapes of a circular cylindrical shell of infinite length having a thickness of radius ratio $\beta = 0{\cdot}05$

(a) First mode

ω_{nl}^*/ω_l^*	C_1	C_3	C_5	C_7	C_9	C_{11}	B_1	B_3	B_5	B_7	B_9	B_{11}
1·00087	0·05	0·16683E−05	0·10759E−09	0·80983E−14	0·39655E−17	−0·9092E−17	−0·5000E−1	−0·55612E−6	−0·21519E−10	−0·11675E−14	0·2257E−17	−0·21138E−18
1·00799	0·15	0·44834E−04	0·25958E−07	0·17616E−10	0·12956E−13	0·13487E−16	−0·1500E+0	−0·14945E−4	−0·51915E−08	−0·25165E−11	−0·144E−14	−0·20949E−17
1·02206	0·25	0·20564E−03	0·32908E−06	0·61697E−09	0·12561E−11	0·26944E−14	−0·2500E+0	−0·68548E−4	−0·65817E−07	−0·88139E−10	−0·140E−12	−0·24656E−15
1·04275	0·35	0·55656E−03	0·17328E−05	0·63163E−08	0·24997E−10	0·10401E−12	−0·3500E+0	−0·18552E−3	−0·34657E−06	−0·90233E−09	−0·278E−11	−0·94581E−14
1·06960	0·45	0·11618E−02	0·59217E−05	0·35305E−07	0·22849E−09	0·15545E−11	−0·4501E+0	−0·38726E−3	−0·11843E−05	−0·50436E−08	−0·254E−10	−0·14132E−12
1·10207	0·55	0·20750E−02	0·15613E−04	0·13726E−06	0·13096E−08	0·13133E−10	−0·5501E+0	−0·69166E−3	−0·31225E−05	−0·19609E−07	−0·146E−09	−0·11939E−11
1·13960	0·65	0·33381E−02	0·34595E−04	0·41844E−06	0·54902E−08	0·75711E−10	−0·6501E+0	−0·11127E−2	−0·69189E−05	−0·59777E−07	−0·610E−09	−0·68828E−11
1·18162	0·75	0·49812E−02	0·67645E−04	0·10709E−05	0·18382E−07	0·33158E−09	−0·7501E+0	−0·16604E−2	−0·13529E−04	−0·15298E−06	−0·204E−08	−0·30144E−10
1·22758	0·85	0·70225E−02	0·12035E−03	0·24014E−05	0·51932E−07	0·11800E−08	−0·8501E+0	−0·23409E−2	−0·24070E−04	−0·34306E−06	−0·577E−08	−1·10727E−09
1·27698	0·95	0·94696E−02	0·19884E−03	0·48560E−05	0·12845E−06	0·35693E−08	−0·9502E+0	−0·31566E−2	−0·39769E−04	−0·69371E−06	−0·143E−07	−0·32448E−09
1·32937	1·05	0·12321E−01	0·30956E−03	0·90357E−05	0·28550E−06	0·94740E−08	−0·1050E+1	−0·41071E−2	−0·61912E−04	−0·12908E−05	−0·317E−07	−0·86128E−09
1·38435	1·15	0·15568E−01	0·45892E−03	0·15703E−04	0·58124E−06	0·22588E−07	−0·1150E+1	−0·51894E−2	−0·91784E−04	−0·22432E−05	−0·646E−07	−0·20535E−08
1·44157	1·25	0·19195E−01	0·65312E−03	0·25776E−04	0·10997E−05	0·49238E−07	−0·1250E+1	−0·63986E−2	−0·13063E−03	−0·36822E−05	−0·122E−06	−0·44762E−08
1·50074	1·35	0·23183E−01	0·89792E−03	0·40315E−04	0·19553E−05	0·99490E−07	−0·1350E+1	−0·77280E−2	−0·17958E−03	−0·57593E−05	−0·217E−06	−0·90446E−08
1·56160	1·45	0·27511E−01	0·11984E−02	0·60503E−04	0·32970E−05	0·18839E−06	−0·1450E+1	−0·91705E−2	−0·23969E−03	−0·86433E−05	−0·366E−06	−0·17126E−07
1·62395	1·55	0·32153E−01	0·15592E−02	0·87612E−04	0·53098E−05	0·33726E−06	−0·1550E+1	−0·10718E−1	−0·31183E−03	−0·12516E−04	−0·590E−06	−0·30660E−07
1·68759	1·65	0·47085E−01	0·19837E−02	0·12298E−03	0·82165E−05	0·57498E−06	−0·1651E+1	−0·12362E−1	−0·39674E−03	−0·17569E−04	−0·913E−06	−0·52271E−07
1·75237	1·75	0·42283E−01	0·24750E−02	0·16798E−03	0·12276E−04	0·93912E−06	−0·1751E+1	−0·14095E−1	−0·49500E−03	−0·23997E−04	−0·136E−05	−0·85374E−07
1·81816	1·85	0·47723E−01	0·30351E−02	0·22397E−03	0·17783E−04	0·14769E−05	−0·1851E+1	−0·15908E−1	−0·60703E−03	−0·31996E−04	−0·198E−05	−0·13426E−06
1·88485	1·95	0·53381E−01	0·36654E−02	0·29231E−03	0·25062E−04	0·22460E−05	−0·1951E+1	−0·17794E−1	−0·73309E−03	−0·41759E−04	−0·279E−05	−0·20418E−06
1·95233	2·05	0·59236E−01	0·43666E−02	0·37430E−03	0·34467E−04	0·33148E−05	−0·2051E+1	−0·19746E−1	−0·87333E−03	−0·53472E−04	−0·383E−05	−0·30134E−06

TABLE 5 Continued

(b) Second mode

ω_{nl}^*/ω_l^*	C_2	C_4	C_6	C_8	C_{10}	C_{12}	B_2	B_4	B_6	B_8	B_{10}	B_{12}
1·00217	0·05	−0·59066E−03	0·86744E−05	−0·14217E−06	0·25151E−08	−0·46707E−10	−0·25017E−1	0·14021E−03	−0·12101E−05	0·11789E−07	−0·10982E−09	0·62141E−12
1·02027	0·15	−0·52904E−02	0·23217E−03	−0·11384E−04	0·60252E−06	−0·33473E−07	−0·75052E−1	0·12555E−02	−0·32364E−04	0·94272E−06	−0·26252E−07	0·44234E−09
1·05605	0·25	−0·14551E−01	0·10559E−02	−0·85799E−04	0·75271E−05	−0·69298E−06	−0·12509E+0	0·34513E−02	−0·14697E−03	0·70873E−05	−0·32652E−06	0·90329E−08
1·10869	0·35	−0·28081E−01	0·28193E−02	−0·31793E−03	0·38717E−04	−0·49467E−05	−0·17514E+0	0·66550E−02	−0·39147E−03	0·26162E−04	−0·16686E−05	0·63141E−07
1·17685	0·45	−0·45421E−01	0·57706E−02	−0·82685E−03	0·12796E−03	−0·20767E−04	−0·22521E+0	0·10752E−01	−0·79871E−03	0·67694E−04	−0·54663E−05	0·25757E−06
1·25867	0·55	−0·65929E−01	0·10037E−01	−0·17316E−02	0·32259E−03	−0·63001E−04	−0·27529E+0	0·15581E−01	−0·13836E−02	0·14086E−03	−0·13631E−04	0·75293E−06
1·35171	0·65	−0·88809E−01	0·15609E−01	−0·31249E−02	0·67531E−03	−0·15291E−03	−0·32540E+0	0·20944E−01	−0·21411E−02	0·25231E−03	−0·28162E−04	0·17449E−05
1·45314	0·75	−0·11316E+00	0·22352E−01	−0·50538E−02	0·12327E−02	−0·31482E−03	−0·37553E+0	0·26617E−01	−0·30483E−02	0·40457E−03	−0·50625E−04	0·33963E−05
1·55997	0·85	−0·13810E+00	0·30038E−01	−0·75127E−02	0·20249E−02	−0·57115E−03	−0·42569E+0	0·32375E−01	−0·40701E−02	0·59573E−03	−0·81733E−04	0·57608E−05
1·66939	0·95	−0·16282E+00	0·38405E−01	−0·10452E−01	0·30614E−02	−0·93793E−03	−0·47588E+0	0·38020E−01	−0·51673E−02	0·82026E−03	−0·12121E−03	0·87368E–05
1·77915	1·05	−0·18670E+00	0·47200E−01	−0·13793E−01	0·43325E−02	−0·14228E−02	−0·52611E+0	0·43398E−01	−0·63035E−02	0·10706E−02	−0·16794E−03	0·12069E−04
1·88760	1·15	−0·20933E+00	0·56218E−01	−0·17450E−01	0·58157E−02	−0·20257E−02	−0·57637E+0	0·48404E−01	−0·74501E−02	0·13387E−02	−0·22031E−03	0·15388E−04
1·99374	1·25	−0·23048E+00	0·65303E−01	−0·21340E−01	0·74818E−02	−0·27406E−02	−0·62666E+0	0·52978E−01	−0·85868E−02	0·16168E−02	−0·27649E−03	0·18268E−04
2·09708	1·35	−0·25004E+00	0·74354E−01	−0·25388E−01	0·93007E−02	−0·35582E−02	−0·67698E+0	0·57096E−01	−0·97013E−02	0·18983E−02	−0·33473E−03	0·20270E−04
2·19746	1·45	−0·26801E+00	0·83311E−01	−0·29536E−01	0·11244E−01	−0·44679E−02	−0·72734E+0	0·60759E−01	−0·10787E−01	0·21777E−02	−0·39346E−03	0·20970E−04
2·29498	1·55	−0·28447E+00	0·92141E−01	−0·33734E−01	0·13287E−01	−0·54585E−02	−0·77773E+0	0·63984E−01	−0·11842E−01	0·24504E−02	−0·45138E−03	0·19974E−04
2·38985	1·65	−0·29951E+00	0·10083E+0	−0·37944E−01	0·15409E−01	−0·65196E−02	−0·82815E+0	0·66792E−01	−0·12866E−01	0·27127E−02	−0·50746E−03	0·16922E−04
2·48236	1·75	−0·31324E+00	0·10939E+0	−0·42136E−01	0·17593E−01	−0·76415E−02	−0·87861E+0	0·69214E−01	−0·13862E−01	0·29616E−02	−0·56088E−03	0·11483E−04
2·57278	1·85	−0·32576E+00	0·11781E+0	−0·46287E−01	0·19825E−01	−0·88151E−02	−0·92910E+0	0·71275E−01	−0·14832E−01	0·31945E−02	−0·61108E−03	0·33509E−05
2·66142	1·95	−0·33720E+00	0·12611E+0	−0·50377E−01	0·22094E−01	−0·10033E−01	−0·97963E+0	0·73005E−01	−0·15778E−01	0·34093E−02	−0·65765E−03	−0·7763E−05
2·74853	2·05	−0·34766E+00	0·13430E+0	−0·54392E−01	0·24390E−01	−0·11286E−01	−0·10302E+1	0·74429E−01	−0·16704E−01	0·36045E−02	−0·70036E−03	−0·2213E−04

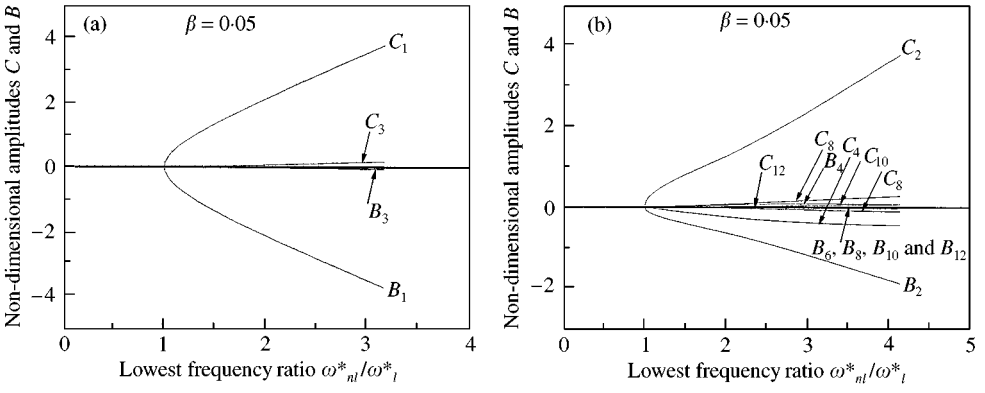

Figure 3. Basic function coefficient contributions to the lowest first (a) and second (b) non-linear modes.

ratio ω^*_{nl}/ω^*_l (ω^*_l is the corresponding linear frequency parameter given in reference [33, p. 39]) is also given in each Table. C_i and B_i represent the contribution of the transverse and circumferential basic functions. It can be seen from Table 5(a) that the coefficient contributions depend on the frequency parameter and the rate of increase in non-linear fundamental frequency with increasing displacement is very low at small amplitudes being about 2% in frequency for an amplitude slightly exceeding 0·14 times the thickness. For the second mode (Table 5(b)), the rate of increase in frequency is about 2%, but for a displacement amplitude up to 0·08 times the shell thickness. This can lead to the conclusion that the practical use of the linear frequencies for such amplitudes can be of acceptable accuracy, although it must limit the frequency estimate accuracy to a reasonable range. However, for displacement amplitudes greater than almost half of the thickness, the increase of fundamental resonance frequencies is about 24%, and the non-linear effect has to be taken into account. For the second mode, the same increase in frequency is obtained for displacement amplitudes greater than, only about a quarter of the thickness.

In Figure 3, the coefficient contributions C_i and B_i of the transverse W^* and circumferential V^* basic functions associated with the lowest first and second modes are plotted versus non-dimensional lowest frequency parameter ratio ω^*_{nl}/ω^*_l (ω^*_l is the corresponding linear frequency parameter given in reference [33, p. 44]). It can be seen that near to the linear frequency of a given mode only the corresponding basic function has a significant contribution. At large amplitudes, the higher order function contributions and resonance frequencies increase.

4.6. TRANSVERSE AND CIRCUMFERENTIAL AMPLITUDE DEPENDENCE OF THE LOWEST FIRST AND SECOND NON-LINEAR MODE SHAPES

The normalized tranverse W^*/W^*_{max} and circumferential V^*/V^*_{max} amplitude of the lowest first and second mode shapes are plotted in Figures 4(a), (b) and 5(a), (b) respectively for the values of the vibration transversal W^*_{max} and circumferential V^*_{max} amplitudes, and values of ω^*_{nl}/ω^*_l are indicated in Tables 6(a), (b). It can be seen that all are amplitude dependent and the non-linearity effect on the transverse displacement is more important than that obtained for the circumferential displacement.

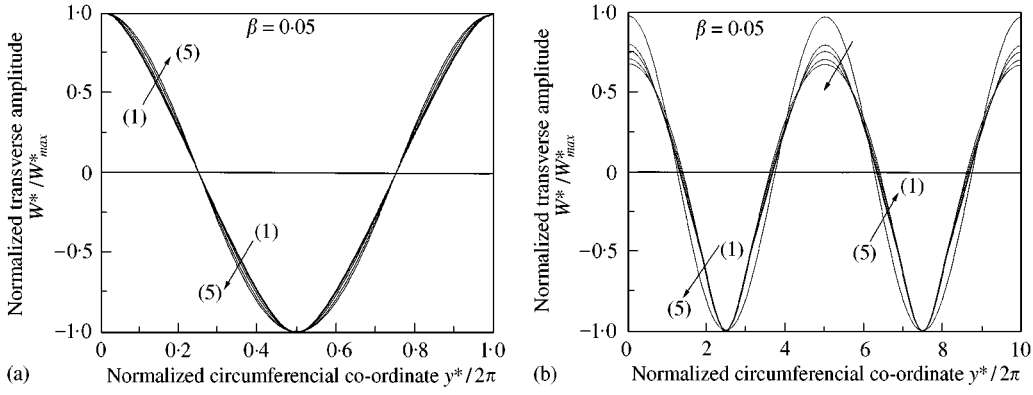

Figure 4. Lowest first (a) and second (b) non-linear modes for the maximum vibration amplitudes presented in Table 6(a) for the first mode and Table 6(b) for the second mode.

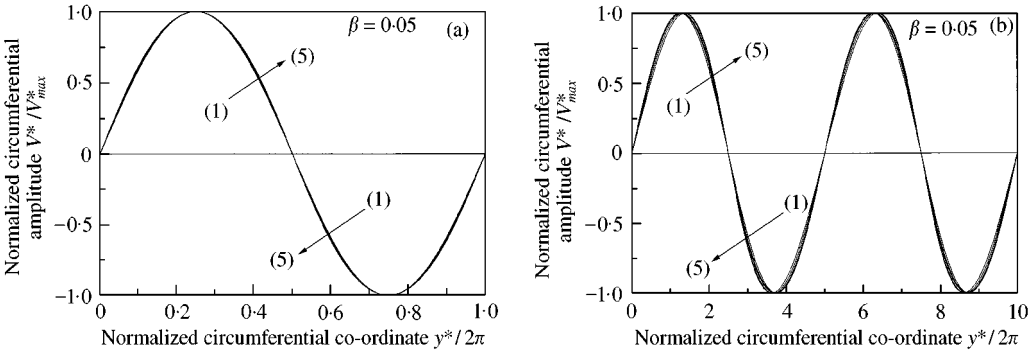

Figure 5. Lowest first (a) and second (b) non-linear modes for the maximum vibration amplitudes presented in Table 6(a) for the first mode and Table 6(b) for the second mode.

TABLE 6

Maximum normalized amplitude and frequency parameter ratio corresponding to the lowest first and second non-linear mode shape and curvatues plotted in Figures 4 *and* 5 ($\beta = 0{\cdot}05$)

Curves	W^*_{max}	V^*_{max}	ω^*_{nl}/ω^*_l
(a) *First mode*			
1	0·02821045	− 0·02815642	1·00086935
2	0·74582949	− 0·72833805	1·47092597
3	1·49561196	− 1·42074741	2·29911678
4	2·26297701	− 2·11159193	3·20647782
5	3·03809808	− 2·80352682	4·14162750
(b) *Second mode*			
1	0·02766874	− 0·00178890	1·00228272
2	0·62406954	− 0·05626903	2·04326994
3	1·28088628	− 0·10706270	3·14706920
4	1·99172875	− 0·15198154	4·14841217
5	2·72706270	− 0·19385251	4·16602541

4.7. CIRCUMFERENTIAL NODAL PATTERNS OF THE LOWEST FIRST AND SECOND NON-LINEAR MODE SHAPES: COMPARISON WITH THE LINEAR CASE

As has been outlined in reference [12], the newcomer to the subject of shell vibration is surprised to find that the fundamental (i.e., lowest frequency) mode of a circular cylindrical shell typically includes many waves around its circumference. In the present work, the fundamental linear mode is given by $W^*(y^*) = (C_i/h)\cos(iy^*)$, when the motion is primarily radial, in which $i = 1$ and y^* varies over the range $[-\pi/2, 3\pi/2]$. This mode is represented in Figure 6, for thickness to radius ratios of 0·05 and 0·09, and for non-dimensional vibration amplitudes equal to 2·05; 5·05 and 7·55, by solid thin lines. The fundamental non-linear modes are represented in the same Figure by dashed lines for the same thickness to radius ratios and vibration amplitudes. It can be seen that this mode is not symmetric and at time t at which $\cos\omega t$ is positive, all points on the right side of the cylinder (A B C) have a positive radial displacement ($w^*(y^*) = \cos y^*$ is positive for y^* between $-\pi/2$ and $\pi/2$) while all points of the left side (C B′ A) have a negative radial displacement ($w^*(y^*) = \cos y^*$ is negative for y^* between $-\pi/2$ and $\pi/2$). The nodal points A and C have always zero radial displacement. As may be expected, at large vibration amplitudes, the first non-linear mode exhibits a slight deformation for small values of β and C_1 (Figure 6(a) corresponding to 0·05 and 2·55 for example), which becomes more pronounced for higher values of β and C_1 (Figure 6(a) corresponding to 0·09 and 7·55 for example), particularly at points corresponding to $y^* = 0$ and π. Similarly, the circumferential nodal patterns of the second non-linear mode shape, when the motion is primarily radial, are represented in Figure 7, for thickness to radius ratios equal to 0·05 and 0·09, and for non-dimensional vibration amplitudes equal to 2·55; 5·05 and 7·55, by dashed lines. The form of the second non-linear

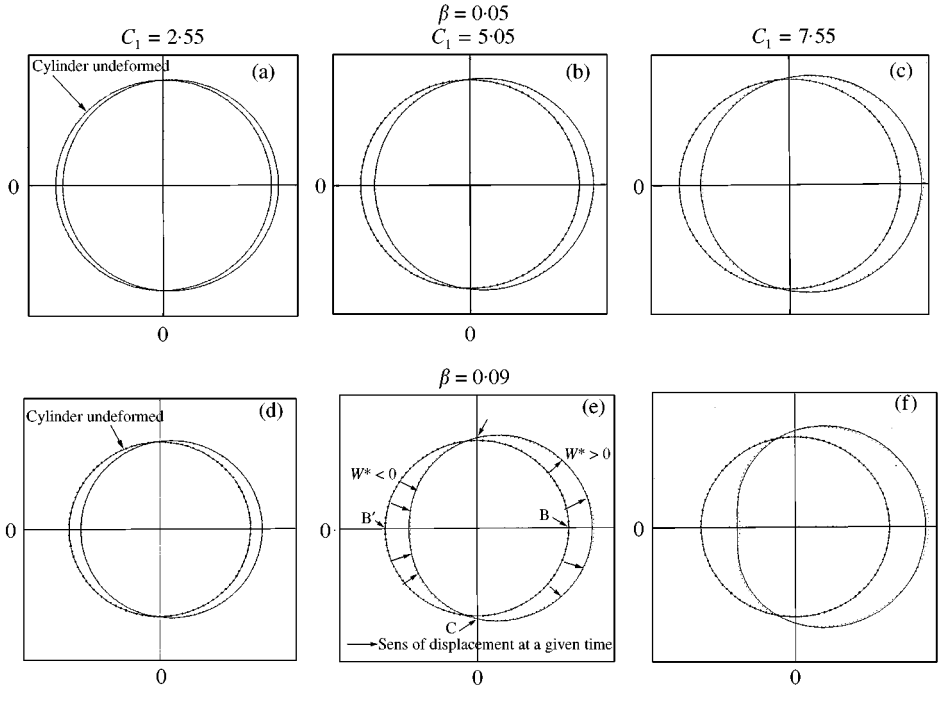

Figure 6. Non-linear (dashed lines) and linear (thin solid lines) circumferential nodal patterns of the lowest first mode shapes for thickness to radius ratios $\beta = 0{\cdot}05$ and 0·09, and non-dimensional vibration amplitude $C_1 = 2{\cdot}55$; 5·05 and 7·55.

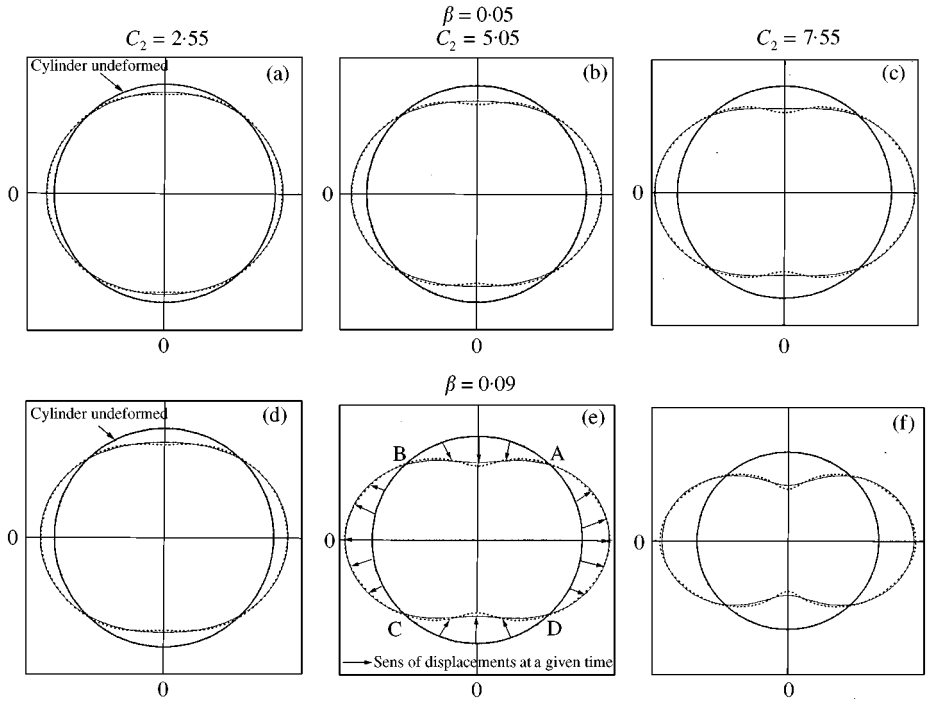

Figure 7. Non-linear (dashed lines) and lines (thin solid lines) circumferential nodal patterns of the lowest second mode shapes for thickness to radius ratios $\beta = 0{\cdot}05$ and $0{\cdot}09$, and non-dimensional vibration amplitude $C_1 = 2{\cdot}55$; $5{\cdot}05$ and $7{\cdot}55$.

mode is symmetric and has four nodal points (ABCD) which have always zero radial displacement. It can be seen in all these Figures that the radial displacement is positive when the circumferential co-ordinate y^* varies over the range $[-\pi/4, \pi/4]$ and $[3\pi/4, 5\pi/4]$, while all points in the ranges $[\pi/4, 3\pi/4]$ and $[5\pi/4, -\pi/4]$ have a negative radial displacement. As has been observed for the first non-linear mode, the form of the second non-linear mode exhibits little deformation for small values of β and C_2 (Figure 7(a) corresponding to $0{\cdot}05$ and $2{\cdot}55$ for example), and the deformation becomes pronounced for higher values of β (Figure 7(f) corresponding to $0{\cdot}09$ and $7{\cdot}55$ for example), in particular, at points corresponding to $y^* = \pi/2$ and $-\pi/2$.

4.8. ANALYSIS OF AXIAL, BENDING AND TOTAL STRESSES ASSOCIATED WITH THE LOWEST FIRST AND SECOND NON-LINEAR MODE SHAPE

The non-dimensional axial, bending and total stress distributions along the cylinder external circumference, associated with the first and second non-linear modes are plotted in Figures 8(a), (b), 9(a), (b) and 10(a), (b) respectively, for various values of the vibration amplitude. It can be observed, for the first non-linear mode, that the axial and total stresses exhibit two maxima at points $y^* = \pi/2$ and $3\pi/2$ and two minima at points $y^* = 2\pi$ and $y^* = \pi$ (Figures 8(a) and 10(a) respectively), and the bending stress exhibits one maximum at point $y^* = 2\pi$ and one minimum at point $y^* = \pi$ (Figure 9(a)). Similarly, for the second non-linear mode, the axial, bending and total stresses present two maxima at points $y^* = 2\pi$ and $y = \pi$ and two minima at points $y^* = \pi/2$ and $y = 3\pi/2$ (Figures 8(b), 9(b) and 10(b) respectively).

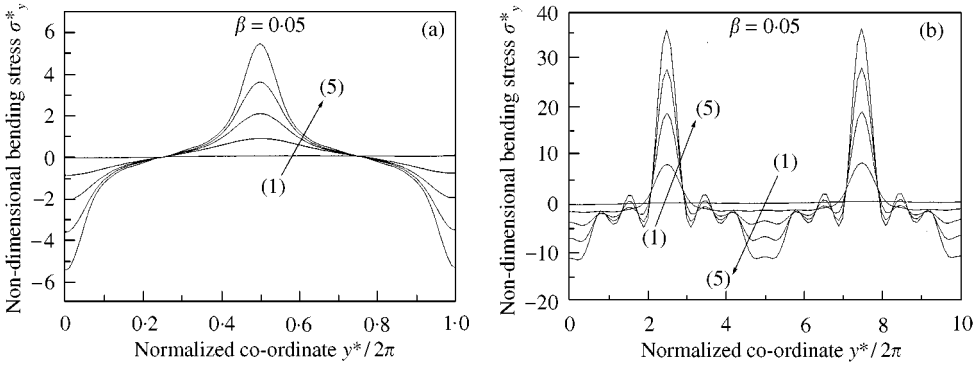

Figure 8. Non-dimensional bending stress distribution along the shell circumference for the lowest first (a) and second (b) non-linear mode for vibration amplitudes equal to curve (1); 0·05, curve (2); 1·30, curve (3); 2·55, curve (4); 3·80, curve (5); 5·05.

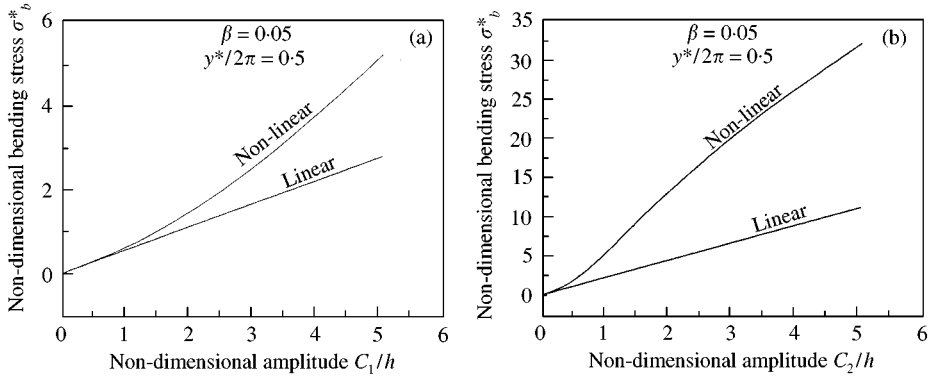

Figure 9. Effect of large vibration amplitudes on the non-dimensional bending stress corresponding to the lowest first (a) and second (b) modes at shell circumference points 0·5 and 0·25 respectively.

The dependence of the non-dimensional non-linear and linear total stresses, computed at point $y^* = 2\pi$ of the shell external circumference, (i.e., $z = h/2$), on the amplitude of vibration is plotted in Figures 11(a), (b), respectively, for both the lowest first and second modes. The linear results were obtained from the present analysis with the non-linear tensors b^*_{ijkl}, b^{*1}_{ijk} and b^{*2}_{ijk} omitted. It can be seen that all curves show amplitude dependence of the stress distribution, and exhibit clearly a high increase of the total stress, compared with the rate of increase expected in the linear theory. Comparing the total stresses corresponding to the first mode obtained when the displacement amplitude C_1 increased from 1 to 4 times the shell thickness, which have the values of 0·000774 and 0·00473 at point $y^* = 2\pi$ (Figure 11(a)) it appears that the rate of increase due to the non-linear effects is 53·3% higher than that predicted in the linear theory. Considering the second mode, the associated bending stress at the point $y^* = 2\pi$ of the shell increased from 0·0262 to 0·116 when the displacement amplitude C_2 increased from 1 to 4 times the thickness (Figure 11(b)). This corresponds to a rate of increase which is 122·5% higher than that predicted by the linear theory.

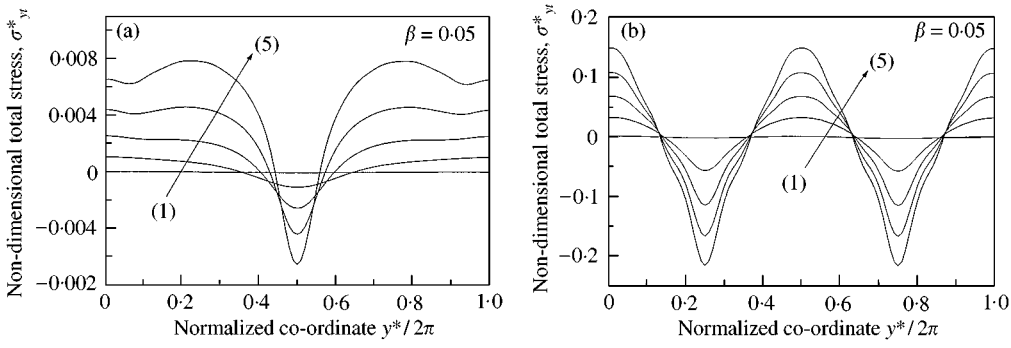

Figure 10. Non-dimensional total stress distribution along the cylinder external circumference, corresponding to the lowest first (a) and second (b) non-linear mode shapes for vibration amplitudes equal to curve (1); 0.05, curve (2); 1.30, curve (3); 2.55, curve (4); 3.8, curve (5); 5.05.

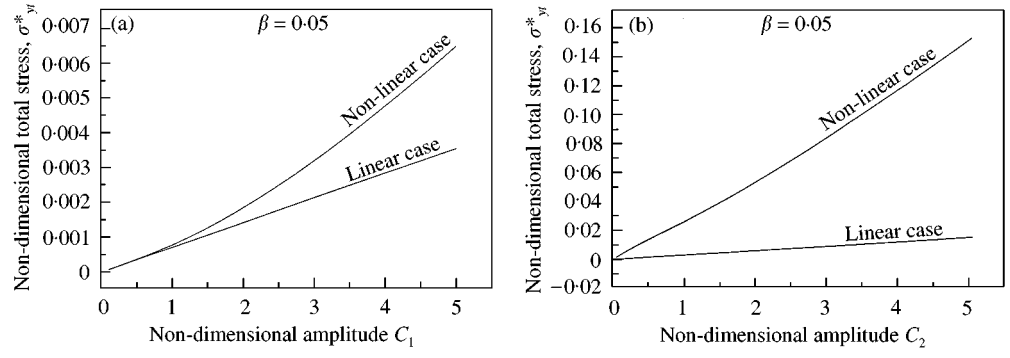

Figure 11. Increase of total stress with increase of vibration amplitude at point of the cylinder external circumference $y^* = 1$, corresonding to the lowest first (a) and second (b) mode shapes. Comparison with the non-linear and linear cases.

5. CONCLUSIONS

The non-linear free response of a circular cylindrical shell of infinite length has been examined by a theoretical model based on Hamilton's principle and spectral analysis, in order to determine the effect of large vibration amplitudes on the first and second coupled transverse–circumferential mode shapes and their corresponding natural frequencies. The coefficient contributions of the transverse and circumferential basic functions corresponding to the lowest frequencies has been determined. The circumferential nodal patterns of the lowest mode shapes and the associated axial, bending and total stress distributions along the cylinder external circumference were studied for various amplitudes of vibration. The validity of the theory and of the numerical results obtained has been established by comparison with previous linear analysis when the vibration amplitudes are very small, with the available previous non-linear results based on the single-mode approach.

The results obtained for the first mode have shown that the rate of increase is about 2% in non-linear frequency for an amplitude slightly exceeding 0·14 times the shell thickness. The same rate of increase has been obtained for the second mode shape but for an amplitude up to 0·08 times the shell thickness. This leads to the conclusion that the practical use of the linear frequencies for such amplitudes can be of acceptable accuracy, although it must limit the frequency estimate accuracy to a reasonable range. However, for displacement

amplitudes greater than almost half of the thickness, the increase of fundamental resonance frequencies is about 24% for the first mode, and the non-linear effect has to be taken into account. For the second mode, the same increase in frequency is obtained for displacement amplitudes greater than only about a quarter of the thickness.

It was also shown that, at large vibration amplitudes, the form of the lowest first non-linear mode exhibits a slight deformation for small values of thickness to radius ratio β and vibration amplitude C_1, and becomes pronounced for higher values, particularly at points corresponding to $y^* = 0$ and π. Similarly, the circumferential nodal patterns of the lowest second non-linear mode shape also exhibits little deformation for small β and C_2, and become pronounced for higher values, particularly at points corresponding to $y^* = \pi/2$ and $-\pi/2$.

Regarding the effect of large vibration amplitudes on the axial, bending and total stress distributions along the cylinder external circumference, associated with these modes, it appears that for the first mode, the axial and total stresses are concentrated at four points: $\pi/2$, $3\pi/2$, 2π and π, and the bending stress is concentrated at two points: 2π and π. For the second mode, the axial, bending and total stresses are concentrated at four points: 2π, π, $\pi/2$ and $3\pi/2$. If is of interest also to note that the rates of increase in the total stress due to the non-linearity effects for the first and second modes is 53 and 122·5% respectively, higher than that predicted in the linear theory, when the displacement amplitude C_1 and C_2 respectively, increase from 1 to 4 times the shell thickness. In both cases, it can be concluded that the non-linearity can affect significantly the total stresses in such types of structure and will certainly modify the predicted fatigue life.

It appears from the present work that the model developed in references [29–32] can be applied not only to beams and plates, but also to shell-type structures, and allows the first and higher order non-linear modes of circular cylindrical shells of infinite length to be estimated quite easily and can be looked upon as an extension, based on a quite simple formulation, of the classical linear eigenvalue problem for free vibration of shells, with a multi-mode approach, with various complicated boundary conditions such as simply supported ends and clamped ends. A parallel extension is being developed for such structures made of new composite materials which will be presented later.

REFERENCES

1. B. A. J. Mustafa and R. Ali 1989 *Computers and Structures* **32**, 355–363. An energy method for free vibration analysis of stiffened circular cylindrical shells.
2. K. T. Chau 1994 *Journal of Applied Mechanics, ASME* **614**, 964–970. Vibrations of transversely isotropic finite circular cylinders.
3. R. N. Arnold and G. B. Warburton 1949 *Royal Society of London., Series A* **197**, 238–256. Flexural vibrations of the walls of thin cylindrical shells having freely supported ends.
4. R. N. Arnold and G. B. Warburton 1953 *Proceedings of the Institution of Mechanical Engineers* **167**, 62–80. The flexural vibration of thin cylinders.
5. G. Coupry 1962 *La Recherche Aeronautique* **91**, 59–65. Vibrations de respiration des cylindres minces. Homogènes ou non.
6. S. B. Dong 1968 *Journal of the Acoustical Society of America* **44**, 1628–1635. Free vibration of laminated orthotropic cylindrical shells.
7. C. W. Bert, J. L. Baker and D. M. Egle 1969 *Journal of Composite Materials* **37**, 480–499. Free Vibration of multilayer anisotropic cylindrical shells.
8. G. B. Warburton and J. Higgs 1970 *Journal of Sound and Vibration* **11**, 335–338. Natural frequencies of thin cantilevered cylindrical shells.
9. M. K. Au-Yang 1978 *Journal of Sound and Vibration* **57**, 341–355. Natural frequencies of cylindrical shells and panels in vacuum and in fluid.
10. J. Mayers and B. G. Wrenn 1966 *Department of Aeronautics and Astronautics, Stanford University, SUDAAR* **269**. On the non-linear free vibrations of thin circular cylindrical shells.

11. T. UEDA 1979 *Journal of Sound and Vibration* **64**, 85–95. Non-linear free vibrations of conical shells.
12. A. W. LEISSA 1984 *Proceeding of the 2nd International Conference on Recent Advances in Structural Dynamics, University of Southampton, Southampton*, Vol. **1**, 241–260. Non-linear analysis of plate and shell vibrations.
13. J. W. TEDESCO, C. N. KOSTEN and A. KALNINS 1987 *Computers and Structures* **25**, 677–685. Free vibration analysis of circular cylindrical shells.
14. K. R. SIVADAS and N. GANESAN 1993 *Journal of Sound and Vibration* **160**, 387–400. Axisymmetric vibration analysis of thick cylindrical shell with variable thickness.
15. T. KOGA and T. KODOMA 1991 *International Journal of Pressure Vessel and Piping* **45**, 223–235. Bifurcation buckling and free vibrations of cylindrical shells under pressure.
16. C. T. F. ROSS, T. JOHNS, S. P. BEEBY and S. F. MAY 1994 *Thin-Walled Structures* **18**, 177–190. Vibration of thin-walled ring-stiffened circular cylinders and cones.
17. K. M. LIEW, C. W. LIM and L. S. ONG 1994 *International Journal of Mechanical Sciences* **36**, 547–565. Flexural vibration of doubly-tapered cylindrical shallow shells.
18. K. M. LIEW and C. W. LIM 1994 *International Journal of Solids and Structures* **31**, 1519–1536. Vibration of perforated doubly-curved shallow shells with rounded corners.
19. K. C. HUNG, K. M. LIEW and M. K. LIM 1995 *Acta Mechanics* **113**, 37–52. Free vibration of cantilevered cylinders: effects of cross-sections and cavities.
20. K. M. LIEW and K. C. HUNG 1995 *International Journal of Solids and Structures* **32**, 3499–3513. Three-dimensional vibratory characteristics of solid cylinders and some remarks on simplified beam theories.
21. K. M. LIEW, K. C. HUNG and M. K. LIM 1995 *Journal of Applied Mechanics* **62**, 159–165. Free vibration studies on stress-free three-dimensional elastic solids.
22. K. M. LIEW, K. C. HUNG and M. K. LIM 1995 *Journal of Applied Mechanics* **62**, 718–724. Vibration of stress-free hollow cylinders of arbitrary cross section.
23. K. M. LIEW, K. C. HUNG and M. K. LIM 1995 *Journal of the Acoustical Society of America* **98**, 1518–1526. Modeling three-dimensional vibration of elliptic bars.
24. L. CHENG and J. NICOLAS 1992 *Journal of Sound and Vibration* **155**, 231–247. Free vibration analysis of a cylindrical shell–circular plate system with general coupling and various boundary conditions.
25. Y. KOBAYASHI and A. W. LEISSA 1995 *International Journal of Non-linear Mechanic* **30**, 57–66. Large amplitude free vibration of thick shallow shells supported by shear diaphragms.
26. K. M. LIEW, K. C. HUNG and M. K. LIM 1997 *Applied Mechanics Review* **50**, 431–444. Vibration of shallow shells: a review with bibliography.
27. M. M. K. BENNOUNA and R. G. WHITE 1984 *Journal of Sound and Vibration* **96**, 309–331. The effects of large vibration amplitudes on the mode shape of a clamped-clamped uniform beam.
28. R. BENAMAR, M. M. K. BENNOUNA and R. G. WHITE 1989 *Proceedings of the 7th International Modal Analysis Conference, Las Vegas, Nevada, U.S.A.* Non-linear mode shapes and resonance frequencies of fully clamped beams and plates.
29. R. BENAMAR 1990 *Ph.D. Thesis, University of Southampton.* Non-linear dynamic behaviour of fully clamped beams and rectangular homogeneous and laminated plates.
30. R. BENAMAR, M. M. K. BENNOUNA and R. G. WHITE 1991 *Journal of Sound and Vibration* **149**, 179–195. The effects of large vibration amplitudes on the mode shapes and natural frequencies of thin elastic structures. Part I: simply supported and clamped–clamped beams.
31. R. BENAMAR, M. M. K. BENNOUNA and R. G. WHITE 1993 *Journal of Sound and Vibration* **164**, 295–316. The effects of large Vibration Amplitudes on the mode shapes and natural frequencies of thin elastic structures. Part II: fully clamped rectangular isotropic plates.
32. R. BENAMAR, M. M. K. BENNOUNA and R. G. WHITE 1990 *Proceeding of the 4th International Conference on Recent Advances in Structural Dynamics, Southampton.* The effects of large Vibration Amplitudes on the mode shapes of a fully clamped, symmetrically laminated, rectangular plates.
33. A. W. LEISSA 1973 *NASA SP-288, Vibration of Shells*, p. 38. Washington, DC: U.S. Government Printing Office.
34. M. STEIN 1964 *NASA Technical Report, TR R-190.* The influence of buckling deformations and stresses on the buckling of perfect cylinders.
35. M. J. D. POWELL 1965 *Computer Journal.* A method for minimising a sum of squares of non-linear functions without calculating derivatives.

36. H. N. CHU 1961 *Journal of the Aerospace Sciences* **28**, 602–609. Influence of large amplitudes on flexural vibrations of thin circular cylindrical shells.

APPENDIX A: NOMENCLATURE

V_b, V_m, V	bending, membrane and total strain energy respectively
T	kinetic energy
y	circumferential position co-ordinate
h	shell thickness
R	shell radius
E	Young's modulus
ρ	mass density
β	thickness to radius ratio h/R
k_{ij}, m_{ji}, b_{ijk}, b_{ijkl}	general terms for the rigidity tensors, the mass tensors, the third non-linearity tensors, and the fourth non-linearity tensors respectively.
k^*_{ij}, n^*_{ji}, b^*_{ijk}, b^*_{ijkl}	general terms for the non-dimensional rigidity tensor, the mass tensor, the third non-linearity tensors, and the fourth non-linearity tensors respectively
$V(y, t)$	circumferential displacement at point y on the shell, $V(y, t) = V(y)\cos \omega t$
$W(y, t)$	transverse displacement at point y on the shell, $W(y, t) = W(y)\cos \omega t$
C_i, B_i $(i = 1, \ldots, n)$	coefficient contributions of the transversal and circumferential basic functions, respectively: $W(y) = C_i W_i(y)$ and $V(y) = B_i V_i(y)$
ω_r	non-linear lowest frequency parameter
ω^*_r	non-dimensional lowest frequency parameter corresponding to ω_r
ω_c	non-linear highest frequency parameter
ω^*_c	non-dimensional highest frequency parameter corresponding to ω_c
ω^*_{nl}/ω^*_l	non-dimensional lowest frequency parameter ratio
ω^*_l	the corresponding lowest linear frequency parameter given in reference [33]
$[B]$	column matrix $[B]^{\mathrm{T}} = [B_1, B_2, \ldots, B_n]$
$[C]$	column matrix $[C]^{\mathrm{T}} = [C_1, C_2, \ldots, B_n]$
$[K]$, $[M]$, $[b]$	rigidity, mass and non-linear matrices respectively
σ, σ^*	stress and non-dimensional stresses respectively
ε^0_i $(i = x, y, z)$, κ_y	in-plane at the mid-surface and bending curvatures respectively the star indicates non-dimensional parameters